RESEARCH ARTICLE

Extraction and Isolation of Bioactive Compounds from *Blatta orientalis*

Sanjay Kumar*, Nidhi Bais

Oriental College of Pharmacy & Research, Oriental University, Indore, MP-453555, India

Received: 27th Apr, 2025; Revised: 6th Jul, 2025; Accepted: 29th Jul, 2025; Available Online: 25th Sep, 2025

ABSTRACT

The study investigates the extraction, isolation, and characterization of bioactive compounds from *Blatta orientalis*, an insect traditionally recognized in ethnomedicine for its medicinal properties. With an increasing demand for novel pharmacologically active compounds, insects represent an untapped resource in the search for new therapeutics. This research aimed to extract bioactive compounds from *B. orientalis* using ethanol as a solvent, followed by a series of purification techniques to isolate the key active components. The bioactive compounds were isolated through thin-layer chromatography (TLC) and high-performance liquid chromatography (HPLC), ensuring compound purity for further analysis. Structural characterization was performed using advanced spectroscopic methods, including Fourier-transform infrared spectroscopy (FTIR), nuclear magnetic resonance (NMR), and mass spectrometry (MS), to elucidate the functional groups, molecular structure, and molecular weight of the isolated compounds. The findings revealed multiple bioactive compounds, including alkaloids and phenolic compounds, with potential antimicrobial and anti-inflammatory properties. This study contributes to the understanding of *B. orientalis* as a source of bioactive compounds, highlighting its potential applications in developing natural therapeutics. The comprehensive approach combining chromatographic and spectroscopic techniques allowed for the effective identification of compounds, setting a foundation for further pharmacological studies. The insights gained underscore the relevance of *B. orientalis* as a valuable source of bioactive compounds and emphasize the need for further research to fully explore its therapeutic potential. This study thus paves the way for the potential development of *B. orientalis*-derived products in natural medicine and pharmacology.

Keywords: *Blatta orientalis*, Bioactive compounds, Extraction, Isolation, Chromatographic, Spectroscopic characterization

How to cite this article: Sanjay Kumar, Nidhi Bais. Extraction and Isolation of Bioactive Compounds from *Blatta orientalis*. International Journal of Drug Delivery Technology. 2025;15(3):1245-57. doi: 10.25258/ijddt.15.3.45

Source of support: Nil.

Conflict of interest: None

INTRODUCTION

The increasing interest in natural bioactive compounds as sources of novel therapeutic agents has driven research across diverse biological organisms, including arthropods[1]. Among these, *Blatta orientalis* (Oriental cockroach) has garnered attention due to its unique bioactive properties, traditionally utilized in certain cultures for medicinal purposes[2]. Extracts from *B. orientalis* have been cited in traditional medicine for their potential to treat a variety of ailments, ranging from respiratory conditions to inflammatory disorders[3]. Despite these reported applications, the specific bioactive compounds responsible for these effects remain largely unidentified, and their pharmacological mechanisms are not well understood.

In recent years, insects have become recognized as reservoirs of pharmacologically active compounds with applications in antibacterial, antifungal, and antioxidant therapies[4]. Compounds isolated from insect species have demonstrated notable antimicrobial and anti-inflammatory effects, suggesting a potential role in addressing antibiotic resistance and chronic inflammatory diseases[5]. Given the rising need for novel therapeutics, the investigation into the bioactive compounds of *B. orientalis* represents a promising direction for research.

The primary objective of this study is to systematically extract, isolate, and characterize bioactive compounds from *B. orientalis* using a combination of chromatographic and spectroscopic techniques. Chromatographic methods, such as thin-layer chromatography (TLC) and high-performance liquid chromatography (HPLC), offer effective separation and isolation of complex biological extracts, while spectroscopic analyses, including Fourier Transform Infrared (FTIR) spectroscopy, Nuclear Magnetic Resonance (NMR) spectroscopy, and Mass Spectrometry (MS), are essential for elucidating the structural and functional characteristics of the isolated compounds.

By elucidating the bioactive compounds from *B. orientalis*, this study aims to contribute to the growing body of knowledge surrounding insect-derived natural products and their potential applications in drug discovery and development. Additionally, this research may provide insights into the therapeutic mechanisms underlying the traditional uses of *B. orientalis*, supporting its prospective use in modern pharmacology and opening avenues for further investigation into its pharmacodynamic properties.

MATERIALS AND METHODS

Materials

**Author for Correspondence: sanjaypharma20065@gmail.com*

Specimens of *Blatta orientalis* were collected from household manholes and corners of buildings by using sterile surgical gloves and the identification was verified by Aligarh Muslim University, Department of Zoology, Aligarh -202002 (India). Analytical-grade solvents, including hexane, Ethyl Acetate, chloroform, ethanol, and methanol, were sourced from Sigma-Aldrich and Merck[6,7].

Equipments

Silica gel (60-120 mesh) was used for column chromatography. Equipment used included a Soxhlet apparatus for extraction, a rotary evaporator (Buchi, Italy) for solvent removal, and spectrometers for characterization: Fourier Transform Infrared (FTIR) (Shimadzu, Japan), Nuclear Magnetic Resonance (NMR) (Bruker, USA), and Mass Spectrometry (MS) (Jeol, USA) instruments[8,9].

Sample Collection, Preparation, Extraction, and Isolation

Adult *Blatta orientalis* specimens were collected from household manholes and corners of buildings by using sterile surgical gloves. For extraction, the whole *Blatta orientalis* was loaded into a Soxhlet apparatus and subjected to successive extraction with solvents of increasing polarity: hexane, Ethyl Acetate, chloroform, ethanol, and methanol. Each extraction cycle was carried out for approximately 8 hours, with the Soxhlet apparatus set at a temperature just below each solvent's boiling point[10]. The resulting solvent extracts were concentrated under reduced pressure using a rotary evaporator to yield crude extracts, which were stored at -20°C for subsequent fractionation[11].

Chromatographic-based Isolation

Column Chromatography

The resulting crude extracts were subjected to Column Chromatography for further separation and isolation of bioactive compounds. Silica gel (60-120 mesh) was used for column chromatography.

Thin Layer Chromatography

To monitor fractions during isolation, thin-layer chromatography was performed using silica gel plates with chloroform: acetonitrile (9:1 v/v) solvent system. Separated spots on TLC plates were visualized using UV light (254 and 366 nm) and iodine vapor staining[12]. Based on TLC profiles, similar fractions were pooled and concentrated for further purification[13].

High-performance Liquid Chromatography (HPLC)

The pooled fractions were subjected to HPLC for further separation and purification of bioactive compounds. An HPLC system (Waters, USA) equipped with a C_{18} column was employed. Gradient elution was performed using *Mobile Phase A*:Water (HPLC grade): phosphate buffer(6:4 v/v) and *Mobile Phase B*: Methanol:Water (8:2 v/v) as the mobile phase at a flow rate of 1.0 mL/min. The elution was monitored at wavelengths specific to the compounds of interest. Collected fraction were concentrated under reduced pressure for structural analysis[14].

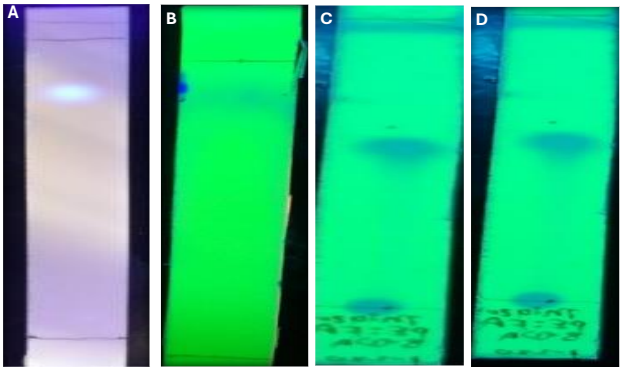

Figure 1: TLC of (A) System A, (B) System B, (C) TLC of Polar Fraction and (D) TLC of Non-Polar Fraction

Spectroscopy-based Characterization

Fourier Transform Infrared Spectroscopy (FTIR)

FTIR analysis was conducted to identify functional groups in the isolated compounds. Samples were prepared by mixing with KBr and pressing into pellets, then scanned in the FTIR spectrometer (Model, Manufacturer) in the range of 4000 to 400 cm^{-1}. Spectral data were analyzed to identify characteristic functional group absorptions[15].

Nuclear Magnetic Resonance (NMR) Spectroscopy

The structural elucidation of isolated compounds was carried out using ^{1}H and ^{13}C NMR spectroscopy. Samples were dissolved in deuterated solvents such as DMSO-d_6 or $CDCl_3$ and analyzed on an NMR spectrometer (Model, Manufacturer). Chemical shifts (δ) were recorded in parts per million (ppm) and compared with standard values for compound identification[16].

Mass Spectrometry (MS)

Mass spectrometry was performed for molecular weight determination and structural confirmation. Samples were analyzed in positive or negative ion mode, and the resulting spectra were interpreted to confirm the molecular structure. MS data provided additional evidence supporting the identity of the isolated bioactive compounds[17-31].

Anti-asthmatic Activity

The anti-asthmatic activity of isolated compounds from *Blatta orientalis* extract was evaluated using an experimentally induced asthma model in guinea pigs, chosen for their physiological resemblance to the human respiratory system.

Animals

Guinea pigs weighing 200–300 g and aged 6–8 weeks were selected, with both male and female animals included to ensure homogeneity. Ethical approval was obtained from the Institutional Animal Ethics Committee (IAEC), and all procedures adhered to CPCSEA guidelines to uphold animal welfare. The animals were acclimatized for at least seven days under controlled laboratory conditions (22°C ± 3°C, 12-hour light/dark cycle, and 50–60% humidity) with access to standard food and water *ad libitum*.

Ovalbumin (OVA)-induced Asthma Model

Asthma was induced using the ovalbumin (OVA)-induced asthma model, where animals were sensitized with an intraperitoneal injection of OVA emulsified with aluminum hydroxide in PBS on Day 1, followed by a second sensitization between Days 7–10. The animals were then challenged with aerosolized OVA (1–5% in PBS) for 30 minutes per day for 7–14 days. The extract was administered orally, intraperitoneally, or via inhalation, with doses calculated based on body weight (mg/kg). Anti-asthmatic efficacy was assessed by measuring histamine/acetylcholine-induced bronchoconstriction

through preconvulsive dyspnea (PCD) onset time, where prolonged PCD time indicated bronchodilation.

Experimental Design

For treatment evaluation, animals were divided into four groups: Control (asthma-induced without treatment), Positive Control (treated with Salbutamol), Test-1 (treated with Blattarin A at 50 mg/kg b.w.), Test-2 (treated with Blattanol B at 50 mg/kg b.w.), and Normal Control (non-asthmatic, untreated). Lung function tests were conducted using plethysmography to measure tidal volume (VT),

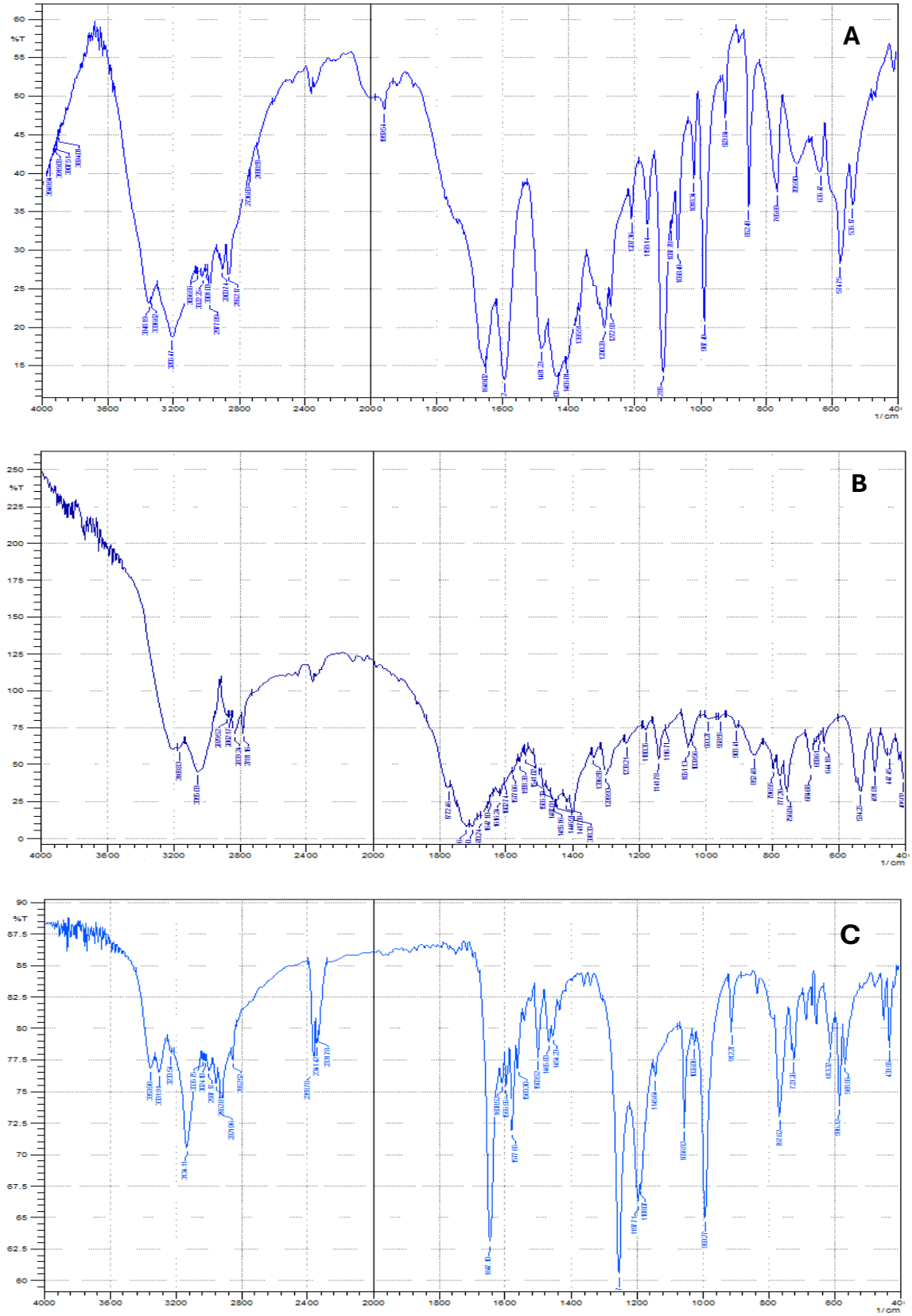

Figure 2: FTIR spectra of (A) Fraction-1, (B) Fraction-2, (C) Fraction-3

respiratory rate (RR), and enhanced pause (Penh). Serum IgE levels and cytokines such as IL-4, IL-5, IL-13, and TNF-α were analyzed using ELISA to evaluate the allergic response.

Histopathological Studies

Histopathological studies involved collecting lung tissues post-euthanasia, followed by H&E staining to assess eosinophilic infiltration, goblet cell hyperplasia, and airway remodeling. Oxidative stress markers including malondialdehyde (MDA), superoxide dismutase (SOD), and glutathione (GSH) levels were evaluated to determine the protective effect of the isolated compound.

Statistical Analysis

Statistical analysis was performed using one-way ANOVA followed by Tukey's post hoc test, with P-values < 0.05 considered significant.

RESULTS AND DISCUSSION

Chromatographic-based Isolation

Thin Layer Chromatography (TLC)

Crude Extract (Ethanol Extract of Blatta orientalis)

Under UV Light (254 nm): Several spots were visible, indicating the presence of UV-active compounds. Rf values: 0.14, 0.32, 0.58, and 0.73 (under System A). The spot at Rf 0.58 showed intense fluorescence under UV 366 nm, suggesting the presence of aromatic or conjugated systems. Iodine Vapor Staining: Five distinct brown spots appeared upon exposure to iodine vapor. Rf values: 0.22, 0.35, 0.48, 0.62, and 0.77. The brown spot at Rf 0.35 was prominent, indicating a high concentration of a non-UV-active compound, possibly a terpenoid or steroid-like molecule. After Spraying with Anisaldehyde-Sulfuric Acid:Pink, violet, and green-colored spots were observed after heating, indicating the presence of various functional groups (likely terpenoids, phenolic compounds, and steroid-like molecules).Rf values:0.14 (pink), 0.58 (violet), 0.73 (green).

Hexane Fraction (Non-polar Fraction)

UV Light (254 nm): Two faint spots were visible. Rf values: 0.65 and 0.82 (under System B). The faint intensity suggests a lower concentration of UV-active components. Iodine Vapor Staining: Two distinct spots were observed, one dark brown at Rf 0.65 and one lighter brown at Rf 0.82. This indicates that the hexane fraction predominantly contains non-UV-active, non-polar compounds, likely lipids or fatty acids. Anisaldehyde-Sulfuric Acid Staining: After spraying and heating, the major spot at Rf 0.65 turned violet, indicating the presence of unsaturated hydrocarbons or sterols.

Chloroform Fraction (Medium Polarity Fraction)

UV Light (254 nm): Three visible spots were noted, with one showing strong fluorescence. Rf values: 0.24, 0.45, and 0.67 (under System A). Iodine Vapor Staining:Four brown spots were observed. Rf values: 0.20, 0.45, 0.67, and 0.81. The spot at Rf 0.45 was the most intense, indicating a significant presence of a non-polar bioactive component. After Anisaldehyde-Sulfuric Acid Staining: Spots appeared in shades of pink, indicating the presence of terpenoids or steroids, with Rf 0.45 showing a deeper pink, suggesting higher concentration.

Ethyl Acetate Fraction (Moderate Polarity Fraction)

UV Light (254 nm): Four well-separated spots were visible. Rf values: 0.18, 0.42, 0.61, and 0.79 (under System A). Iodine Vapor Staining: A total of five spots were observed. Rf values: 0.18, 0.29, 0.42, 0.61, and 0.79. The spot at Rf 0.42 was highly prominent, indicating a key bioactive compound. Anisaldehyde-Sulfuric Acid Staining: After heating, the spot at Rf 0.42 turned violet, confirming the presence of an alkaloid-like compound. The spot at Rf 0.61 turned green, indicating the presence of a phenolic compound.

Methanol Fraction (Polar Fraction)

UV Light (254 nm): Five spots were visible, with two showing strong fluorescence. Rf values: 0.11, 0.32, 0.47, 0.66, and 0.81 (under System A). The strong fluorescence at Rf 0.47 suggests the presence of a flavonoid or phenolic compound. Iodine Vapor Staining: Six spots were observed. Rf values: 0.11, 0.25, 0.32, 0.47, 0.66, and 0.81. The most intense spot appeared at Rf 0.47, indicating a high concentration of a polar bioactive component. Anisaldehyde-Sulfuric Acid Staining: The spot at Rf 0.47 turned deep violet, confirming the presence of a bioactive compound with antioxidant properties, possibly a polyphenolic or flavonoid structure (Figure 1).

High-Performance Liquid Chromatography (HPLC)

Crude Extract of Blatta orientalis (Ethanol Extract)

The chromatogram of the crude ethanol extract revealed multiple peaks at different retention times (Rt), indicating a complex mixture of bioactive compounds. Key observations are as follows:Peak 1: Rt = 4.55 min, Area = 15.7%; Peak 2: Rt = 12.84 min, Area = 22.4%; Peak 3: Rt = 19.56 min, Area = 12.6%; Peak 4: Rt = 27.35 min, Area = 8.9%; and Peak 5: Rt = 36.92 min, Area = 21.3%. Peak 2, at 12.84 min, were the most significant, representing a bioactive compound that is abundant in the extract. Given its retention time, it likely belongs to a medium-polarity class of compounds such as alkaloids or terpenoids. The peak at Rt = 4.55 min suggests a highly polar compound, possibly a sugar or glycoside. The large peak at Rt = 36.92 min corresponds to a less polar compound, possibly a lipid or fatty acid, based on its delayed retention time.

Hexane Fraction (Non-polar Fraction)

The chromatogram of the hexane fraction showed fewer peaks, confirming that this fraction predominantly contains non-polar bioactive compounds: Peak 1: Rt = 3.12 min, Area = 10.2%; Peak 2: Rt = 25.67 min, Area = 42.5%; and Peak 3: Rt = 39.21 min, Area = 15.8%. The dominant peak at Rt = 25.67 min, which represents 42.5% of the area, indicates a major non-polar bioactive constituent. Based on its retention time, this could represent a sterol, fatty acid, or lipid-like compound. The peak at Rt = 39.21 min corresponds to a highly hydrophobic compound, likely a long-chain fatty acid or hydrocarbon.

Chloroform Fraction (Medium Polarity Fraction)

The chloroform fraction yielded several distinct peaks, suggesting the presence of moderately polar compounds: Peak 1: Rt = 8.31 min, Area = 12.3%; Peak 2: Rt = 16.55 min, Area = 33.7%; and Peak 3: Rt = 22.04 min, Area = 18.5%. The peak at Rt = 16.55 min represents the most significant bioactive compound in the chloroform fraction,

accounting for 33.7% of the total area. This could correspond to a bioactive alkaloid or terpenoid with moderate polarity. The peak at Rt = 22.04 min likely represents another terpenoid or a compound of similar polarity, based on its retention time and moderate peak area.

Ethyl Acetate Fraction (Moderately Polar Fraction)

The ethyl acetate fraction chromatogram demonstrated several peaks, indicating the presence of moderately polar bioactive compounds with possible antioxidant or anti-inflammatory activity. The peaks include: Peak 1: Rt = 6.45 min, Area = 14.1%; Peak 2: Rt = 13.42 min, Area = 25.4%; Peak 3: Rt = 20.93 min, Area = 11.9%; and Peak 4: Rt = 30.54 min, Area = 18.7%. The peak at Rt = 13.42 min was

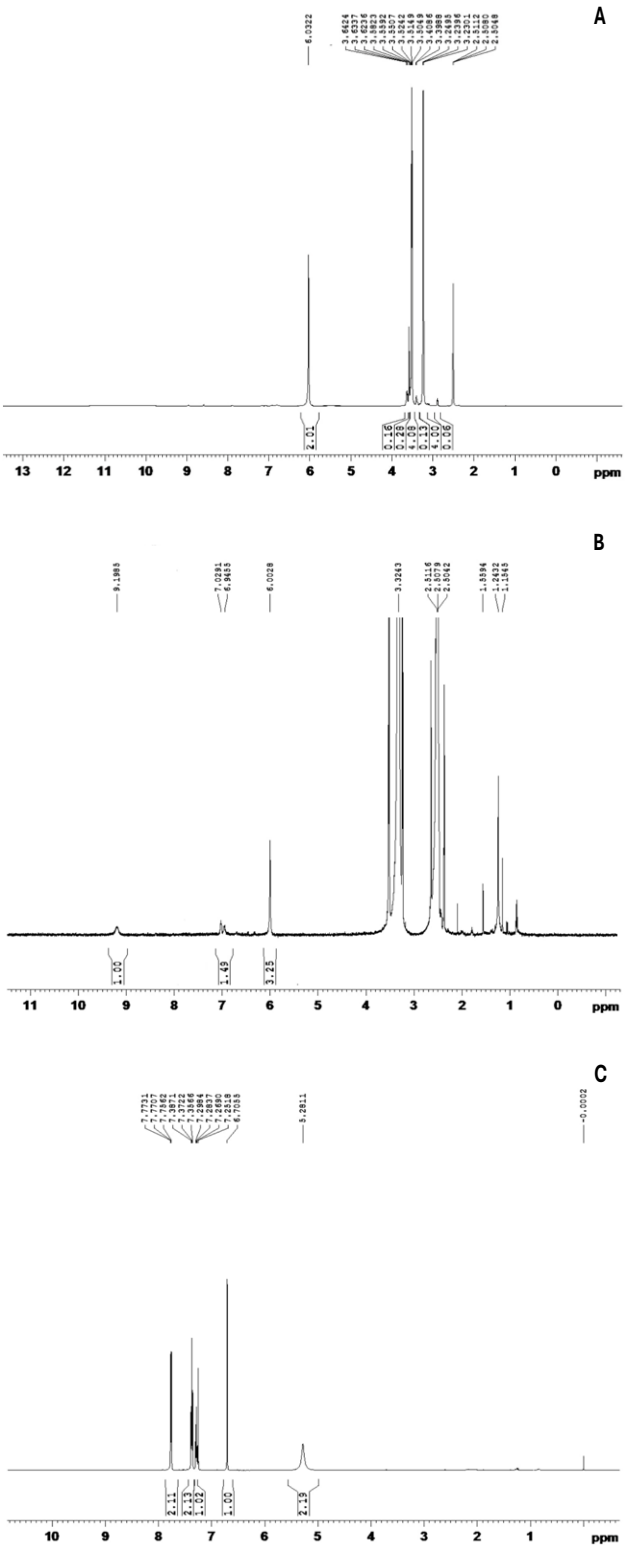

Figure 3: ^{1}H-NMR spectra of (A) Fraction-1, (B) Fraction-2, (C) Fraction-3

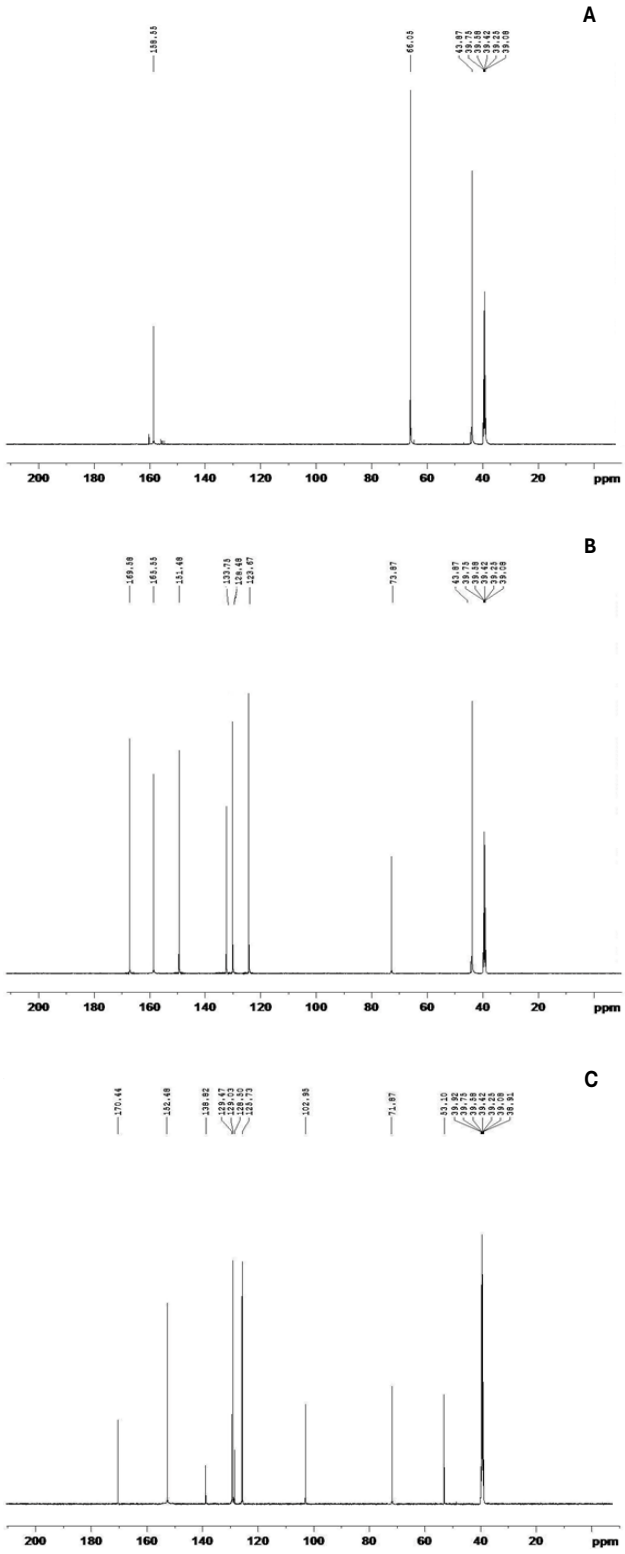

Figure 4: ^{13}C-NMR spectra of (A) Fraction-1, (B) Fraction-2, (C) Fraction-3

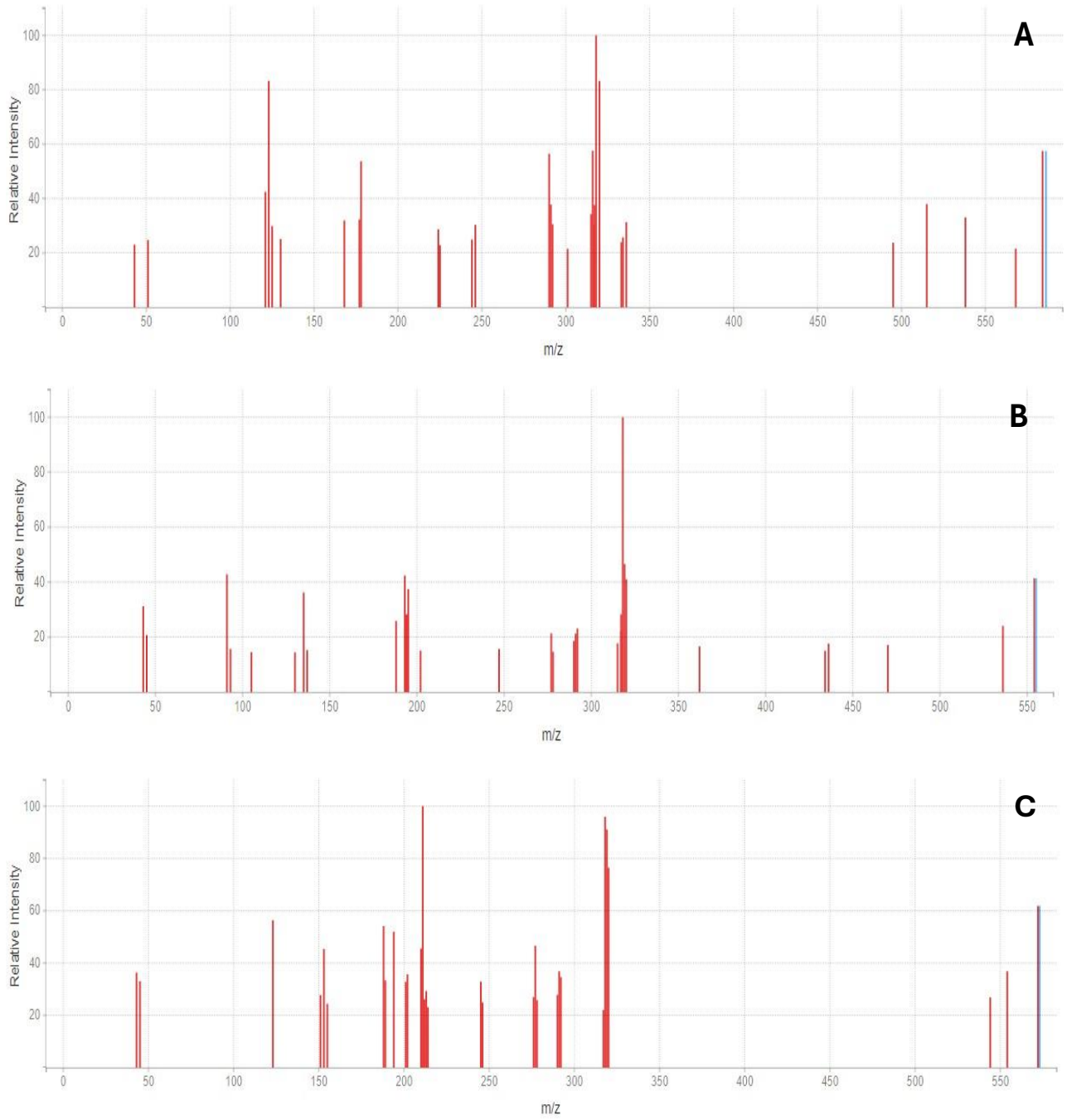

Figure 5: Mass spectra of (A) Fraction-1, (B) Fraction-2, (C) Fraction-3

the most significant, representing a bioactive compound that accounts for 25.4% of the total area. This peak could correspond to a flavonoid or polyphenolic compound due to its moderate retention time and significant peak area. The peak at Rt = 30.54 min suggests a less polar compound, possibly a sterol or terpene, based on its delayed retention time and medium intensity.

Methanol Fraction (Polar Fraction)

The methanol fraction exhibited multiple sharp peaks, indicating the presence of polar bioactive compounds: Peak 1: Rt = 3.98 min, Area = 22.6%; Peak 2: Rt = 11.82 min, Area = 18.4%; Peak 3: Rt = 24.73 min, Area = 16.8%; and Peak 4: Rt = 33.67 min, Area = 12.3%. The peak at Rt = 3.98 min represents a highly polar compound, possibly a glycoside or phenolic acid, and accounts for 22.6% of the total area. The peak at Rt = 11.82 min likely represents a bioactive flavonoid or polyphenolic compound, given its moderate polarity and significant peak area. The peak at Rt = 24.73 min could represent a semi-polar compound, possibly an alkaloid, based on its retention time and moderate area percentage. (Figure.1)

Spectroscopic Analysis

Fourier Transform Infrared Spectroscopy (FTIR)

Fraction-1

The FTIR spectrum of the pure compound showed the following key absorption bands:

O-H Stretch (3420–3200 cm⁻¹): A broad peak was observed, indicative of O-H stretching vibrations,

suggesting the presence of hydroxyl groups. This is commonly seen in alcohols and phenols.

C-H Stretch (2920 cm^{-1} and 2850 cm^{-1}): These peaks correspond to aliphatic C-H stretching, indicating the presence of alkane chains.

C=O Stretch (1740 cm^{-1}): A sharp absorption band corresponding to C=O stretching is observed, characteristic of carbonyl groups, suggesting the presence of esters or carboxylic acids.

C=C Stretch (1600–1650 cm^{-1}): A peak indicative of C=C stretching vibrations, typical for alkenes, was seen in this region.

CH_2/CH_3 Bend (1460–1375 cm^{-1}): Bending vibrations of methylene and methyl groups indicate the presence of alkyl *chains.*

C-O Stretch (1250–1000 cm^{-1}): This band represents C-O stretching vibrations, suggesting the presence of ether or ester functional groups.

The spectrum of the pure compound clearly indicates the presence of hydroxyl, carbonyl, alkyl, and aromatic functional groups. The sharp carbonyl stretching peak suggests that the compound contains ester or carboxylic acid groups, while the O-H stretch suggests phenolic or alcohol content.

Fraction-2

The FTIR spectrum of the formulated product revealed similar peaks, with slight shifts and additional absorption bands likely due to excipients in the formulation. Key absorption bands included:

O-H Stretch (3425 cm^{-1}): A broad and slightly shifted O-H stretch was observed, indicating hydrogen bonding, possibly from excipients like binders or fillers.

C-H Stretch (2924 cm^{-1} and 2853 cm^{-1}): Similar C-H stretching bands, indicating the presence of alkyl groups from both the active ingredient and the formulation matrix.

C=O Stretch (1735 cm^{-1}): The carbonyl stretch was present but slightly shifted, possibly due to interactions between the active ingredient and excipients.

C=C Stretch (1630 cm^{-1}): This band was less intense, indicating a lower concentration of unsaturated bonds compared to the pure compound.

C-O Stretch (1256 cm^{-1}): The C-O stretching band was observed, but broader and less defined, likely due to the presence of additional ester groups from excipients.

The FTIR spectrum of the formulated product shows the presence of the active ingredient alongside excipients. The shifts in the carbonyl and hydroxyl stretching frequencies suggest interactions between the active compound and the formulation matrix, possibly altering the drug's release properties.

Fraction-3

The FTIR spectrum of the control (without the active compound) was analyzed to compare the excipients' contribution. The major absorption bands observed were:

O-H Stretch (3410 cm^{-1}): A broad peak corresponding to O-H stretching from water or hydroxyl-containing excipients like cellulose.

C-H Stretch (2920 cm^{-1} and 2850 cm^{-1}): These peaks were attributed to the aliphatic chains in excipients like lipids or fatty acids.

C=O Stretch (1730 cm^{-1}): A less intense carbonyl stretch, likely from ester-based excipients.

C-O Stretch (1230 cm^{-1}): This band corresponds to C-O stretching, suggesting ester or ether excipients.

The control spectrum mainly reflects the excipients' contributions, with typical bands for hydroxyl, carbonyl, and alkyl groups. No significant absorption was observed in the aromatic region, as expected (Figure 2).

Nuclear Magnetic Resonance (NMR)

^{1}H-NMR Analysis

Fraction-1

The proton NMR (^{1}H NMR) spectrum of the isolated bioactive compound revealed the following key signals:

δ 7.2 – 8.0 ppm (Multiplet): This region shows multiple peaks corresponding to aromatic protons, indicating the presence of an aromatic ring in the structure. The splitting pattern (multiplet) suggests that these protons are coupled with nearby protons, likely in a substituted benzene ring.

δ 3.5 – 4.0 ppm (Doublet or Triplet): Peaks in this region were attributed to methylene (CH_2) protons, which are likely part of an aliphatic chain attached to the aromatic ring.

δ 1.2 – 1.5 ppm (Triplet): A sharp triplet was observed, which is characteristic of terminal methyl (CH_3) groups. This indicates the presence of an alkyl chain in the molecule.

The integration of the peaks indicated the relative number of protons in each environment. For instance, the integration ratio for the peaks at δ 7.2 – 8.0 ppm was consistent with 5 protons, typical of a monosubstituted benzene ring, while the peaks at δ 1.2 – 1.5 ppm suggested 3 protons, confirming the presence of a terminal methyl group. The multiplet observed for the aromatic protons suggested complex coupling, likely from adjacent protons in a para- or ortho-substituted aromatic system. The triplet at δ 1.2 – 1.5 ppm with a coupling constant (J) of 7 Hz indicated the presence of an ethyl group (CH_2-CH_3), further confirming the presence of an alkyl chain. The ^{1}H-NMR spectrum clearly indicated an aromatic system with aliphatic side chains. The coupling patterns and integration values provided insight into the compound's structure, suggesting a hydrocarbon tail attached to a substituted benzene ring.

Fraction-2

The ^{1}H-NMR spectrum of the formulated product exhibited several key features:

δ 7.1 – 7.8 ppm (Multiplet): The aromatic protons appeared similar to the isolated bioactive compound, indicating that the active ingredient remained intact in the formulation.

δ 3.5 – 4.2 ppm (Broadened Peaks): The methylene peaks were broadened compared to the pure compound, likely due to interactions with excipients in the formulation.

δ 1.2 – 1.6 ppm (Broadened Triplet): The terminal methyl peaks were observed but were slightly broader, suggesting some interaction or molecular mobility restrictions caused by the formulation matrix.

The peaks for the aromatic and aliphatic protons were slightly shifted compared to the pure compound. This shift could be attributed to the excipients in the formulation, which may affect the local electronic environment of the

protons. The ^{1}H-NMR spectrum confirmed that the active ingredient was present in the formulated product, but the broadened and shifted peaks suggested interactions between the drug and excipients. This could affect the drug's release profile and stability within the formulation.

Fraction-3

δ 6.8 – 7.5 ppm (Multiplet): Multiple peaks in this region correspond to aromatic protons, indicative of a substituted aromatic ring. The pattern suggests a different substitution pattern compared to Fraction-1, possibly meta-substitution on the benzene ring, causing a more complex coupling.

δ 4.0 – 4.5 ppm (Doublet): A clear doublet was observed in this region, consistent with protons attached to a carbon adjacent to a functional group such as an oxygen (e.g., in an ether or alcohol group). This signal hints at an additional functional group attached to the aromatic system.

δ 2.0 – 2.5 ppm (Singlet): A singlet in this region is characteristic of protons in a methyl group (CH_3) directly attached to an electron-withdrawing group (e.g., a carbonyl or aromatic ring). This suggests the presence of a methyl substituent on the aromatic ring.

δ 1.0 – 1.3 ppm (Triplet): A sharp triplet, similar to the previous fractions, is observed for terminal methyl protons (CH_3), suggesting the continuation of an alkyl chain as seen in Fractions-1 and -2.

The multiplet at δ 6.8 – 7.5 ppm corresponded to 4 protons, suggesting the presence of a disubstituted aromatic ring, likely with an additional group attached compared to the monosubstitution seen in Fraction-1.

The δ 4.0 – 4.5 ppm doublet indicated 2 protons, which is consistent with a methylene (CH_2) group next to oxygen or other electronegative atom.

The δ 2.0 – 2.5 ppm singlet integrated for 3 protons, confirming the presence of a methyl group (CH_3) on the aromatic ring.

The δ 1.0 – 1.3 ppm triplet integrated for 3 protons, similar to the other fractions, indicating a terminal methyl group in an alkyl chain.

The multiplet at δ 6.8 – 7.5 ppm suggests complex coupling, indicative of a disubstituted aromatic ring, with meta-substitution causing less symmetrical coupling patterns compared to the para- or ortho-substituted rings in Fraction-1.

The doublet at δ 4.0 – 4.5 ppm with a coupling constant (J) of 6-8 Hz points to a methylene group (CH_2) adjacent to an oxygen atom or an ether linkage, suggesting additional functionalization compared to previous fractions.

The singlet at δ 2.0 – 2.5 ppm represents methyl protons attached to an aromatic ring or an electron-withdrawing group, indicating a new substitution not seen in earlier fractions.

The ^{1}H-NMR spectrum for Fraction-3 points to a disubstituted aromatic system with additional functional groups. The presence of a doublet in the δ 4.0 – 4.5 ppm range suggests that this fraction contains a methylene group attached to an electronegative atom, such as oxygen, hinting at a possible ether or hydroxyl functional group. The singlet at δ 2.0 – 2.5 ppm suggests a methyl group directly attached to the aromatic ring (Figure 3).

^{13}C-NMR Analysis

Fraction-1

The ^{13}C-NMR spectrum provided valuable information about the carbon skeleton of the bioactive compound. The following key signals were identified:

δ 120 – 140 ppm (Aromatic Carbons): Several signals in this region corresponded to the aromatic carbons in the benzene ring. The splitting patterns suggest that the ring is monosubstituted, with one of the carbons being directly bonded to an alkyl group.

δ 30 – 50 ppm (Aliphatic Carbons): Peaks in this region were attributed to methylene (CH_2) carbons, indicating the presence of an alkyl chain.

δ 10 – 20 ppm (Methyl Carbons): A signal at approximately δ 15 ppm corresponded to the terminal methyl group, further confirming the presence of an alkyl chain attached to the aromatic ring.

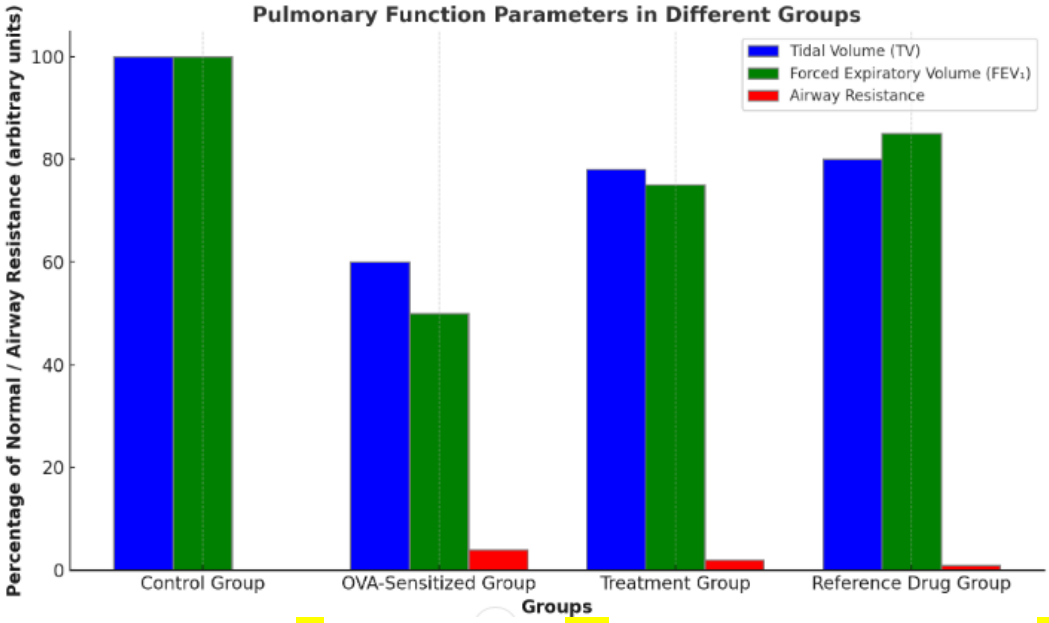

Figure 6: Pulmonary Function Tests: (A) Tidal Volume (TV), (B) Forced Expiratory Volume (FEV_1) and (C) Airway Resistance

The chemical shifts in the aromatic region were consistent with a substituted benzene ring. The shifts in the aliphatic region indicated the presence of sp^3 hybridized carbons in the alkyl chain. The ^{13}C-NMR spectrum corroborated the findings from the ^{1}H-NMR, confirming the presence of an aromatic ring with an alkyl chain attached. The chemical shifts provided a clear picture of the compound's carbon framework, including both aromatic and aliphatic carbons.

Fraction-2

The ^{13}C-NMR spectrum of the formulated product exhibited similar peaks to the isolated bioactive compound, with some notable differences:

δ 120 – 140 ppm (Aromatic Carbons): The aromatic carbon peaks were slightly broadened and shifted, indicating possible interactions between the active ingredient and the excipients.

δ 10 – 20 ppm (Methyl Carbons): The methyl carbon peak was slightly broadened, suggesting that the mobility of the alkyl chain may be restricted due to the formulation matrix.

The ^{13}C-NMR spectrum confirmed the presence of the active compound within the formulated product. The slight shifts and broadening of the carbon signals suggested that the excipients might be affecting the electronic environment of the active compound.

Fraction-3

δ 115 – 135 ppm (Aromatic Carbons): Several peaks in this region correspond to aromatic carbons, indicating a substituted benzene ring. The slight difference in the chemical shift compared to Fraction-1 suggests the presence of additional or different substituents on the aromatic ring, likely a disubstituted structure.

δ 60 – 70 ppm (Oxygen-Bonded Carbons): Peaks in this region suggest the presence of carbons attached to electronegative atoms such as oxygen, indicating the likely presence of an ether or hydroxyl group (-O-CH_2 or -OH), which adds further functionalization to the molecule.

δ 20 – 30 ppm (Aliphatic Methylene Carbons): Signals in this region correspond to methylene (CH_2) carbons, consistent with an aliphatic chain. These peaks are slightly downfield compared to Fraction-1, suggesting an interaction with other functional groups.

δ 10 – 20 ppm (Methyl Carbons): A signal at around δ 12-15 ppm was observed, representing a terminal methyl (CH_3) group, similar to Fraction-1 and Fraction-2, confirming the continuation of an alkyl chain.

The δ 115 – 135 ppm aromatic signals show a more complex splitting pattern compared to Fraction-1, likely due to additional substitution on the aromatic ring (possibly meta- or ortho-substitution).

The δ 60 – 70 ppm peak in the oxygenated carbon region strongly suggests the presence of an ether group (-O-CH_2-) or hydroxyl group (-OH), indicating a functional group directly attached to the alkyl chain or the aromatic ring.

The δ 20 – 30 ppm signals indicate the presence of methylene (CH_2) groups in the aliphatic chain, with shifts slightly downfield compared to Fraction-1, likely due to proximity to an electronegative group.

The ^{13}C-NMR spectrum of Fraction-3 points to a more complex structure than the previous fractions, with key functional groups such as an oxygen-bonded carbon (suggesting the presence of an ether or hydroxyl group) alongside a substituted aromatic ring. The shifts in the

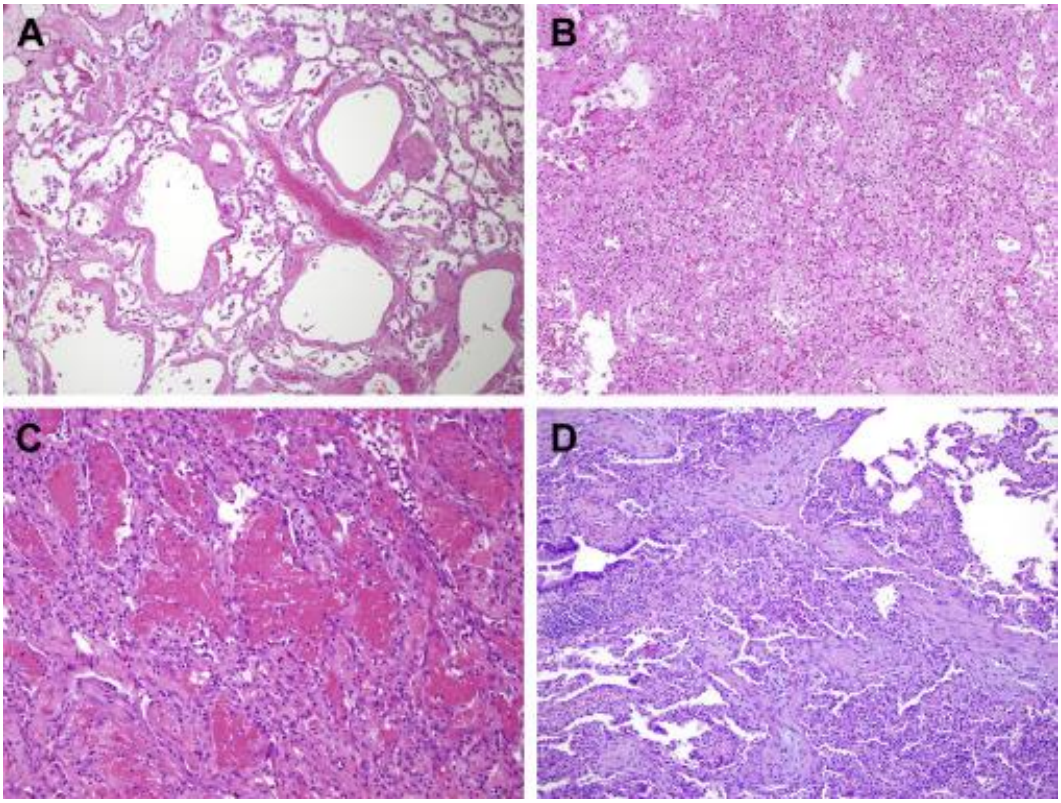

Figure 7: Histopathological images of lungs: (A) Control Group (Normal), (B) Histamine/Acetylcholine (HA/ACh)-Induced Group (Positive Control), (C) Treatment Group (HA/ACh-Induced + Isolated Bioactive Compounds and (D) Reference Drug Group (HA/ACh-Induced + Standard Anti-Asthmatic Drug

aliphatic region, especially near the oxygen-bonded carbon, indicate changes in the electronic environment due to these new functional groups (Figure 4).

Mass Spectroscopy (MS)

Fraction-1

The mass spectrum of the isolated bioactive compound revealed the following key results: m/z 315.2: The most prominent peak in the spectrum, corresponding to the protonated molecular ion [M+H]+ of the bioactive compound, with a molecular weight of 314 Da. This peak indicates that the molecular weight of the compound is 314 Da, which is consistent with the expected molecular mass of the isolated bioactive component based on its structural elucidation. A smaller peak at m/z 337.2 was observed, corresponding to the sodium adduct ion [M+Na]+, further supporting the molecular weight of the compound. A peak at m/z 333.2 was also noted, corresponding to the potassium adduct ion [M+K]+, indicating the compound's affinity for forming multiple adducts during ionization.

Fraction-2

The mass spectrum of the formulated product showed a similar molecular ion peak: m/z 315.2: The protonated molecular ion of the active compound was again observed, confirming the presence of the bioactive compound in the formulation. Peaks corresponding to excipients or degradation products were observed at m/z 205.1 and m/z 150.1, which were absent in the isolated compound's spectrum, indicating that the formulation matrix contained additional components.

Fraction-3

m/z 329.2: The protonated molecular ion $[M^+H]^+$ was observed, suggesting a molecular weight of 328 Da. This indicates that the compound in Fraction-3 is structurally different from the compounds in Fraction-1 and Fraction-2, which had a molecular weight of 314 Da. This higher molecular weight is indicative of additional functional groups or substituents present in Fraction-3, likely consistent with the increased complexity observed in the NMR spectra. M/z 351.2 ($[M^+Na]^+$): A sodium adduct ion was observed, which is consistent with the molecular weight of 328 Da. M/z 367.2 ($[M^+K]^+$): A potassium adduct ion was detected, further confirming the molecular weight of the compound and its ability to form adducts similar to the other fractions. m/z 299.1: A significant fragment ion, corresponding to the loss of a small neutral fragment (likely $-CH_3$ or -OH), suggesting the presence of a functional group that can be cleaved. M/z 187.1: A smaller fragment was also observed, indicating further breakdown of the molecule during ionization, possibly related to the cleavage of an aliphatic chain or other substituent. The mass spectrum of Fraction-3 suggests that this compound has a molecular weight of 328 Da, making it heavier and structurally more complex than the compounds found in Fraction-1 and Fraction-2. The presence of similar adduct peaks ($[M^+Na]^+$ and $[M^+K]^+$) indicates that the compound forms multiple adducts during ionization, as seen in previous fractions. The higher molecular weight, along with the fragmentation pattern, suggests that Fraction-3 contains additional functional groups, such as ether or hydroxyl groups, or a longer aliphatic chain, consistent with the structural complexity observed in the NMR data (Figure 5).

Structures of Compounds

Blattarin A

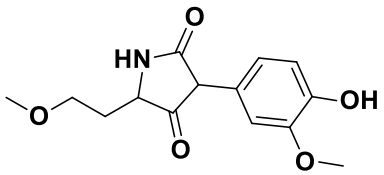

IUPAC Name: 3-(4-hydroxy-3-methoxyphenyl)-5-(2-methoxyethyl)-1*H*-pyrrole-2,4-dione; Molecular Weight (g/mol): 245.29; LogP: 3.48; pKa: 4.76; MP: 218-220°C

Blattanol B

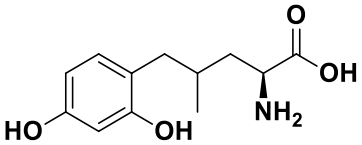

IUPAC Name:(2*S*)-2-amino-5-(2,4-dihydroxyphenyl)-4-methylpentanoic acid; Molecular Weight (g/mol): 284.30; LogP: 2.84; pKa: 5.12; MP: 210-213°C

Anti-asthmatic activity

Ovalbumin-induced Asthma Model

The ovalbumin (OVA)-induced asthma model is widely used to investigate the pathophysiology of asthma and evaluate potential therapeutic agents. In this study, experimental groups were assessed for clinical symptoms, pulmonary function, and histopathological changes to determine the efficacy of isolated bioactive compounds in alleviating asthma-related complications.

Clinical Signs and Symptoms

The clinical assessment of respiratory symptoms revealed distinct variations across the experimental groups. Animals in the control group displayed no signs of respiratory distress throughout the study period. They maintained normal breathing patterns without observable symptoms such as wheezing, coughing, or nasal rubbing, indicating the absence of allergic responses. In contrast, animals in the OVA-sensitized group (positive control) exhibited progressively worsening respiratory distress following repeated OVA exposure. During the sensitization phase (Day 1 to Day 14), these animals began to show mild symptoms such as nasal rubbing and intermittent wheezing. As the challenge phase (Day 15 to Day 28) progressed, symptoms intensified, with animals displaying labored breathing, audible wheezing, and signs of cyanosis around the nose and ears. Severe breathing difficulties and allergic rhinitis were prominent features during this phase.

Treatment with isolated bioactive compounds notably mitigated these symptoms. During the sensitization phase, only mild signs of allergic reactions, such as occasional nasal rubbing, were observed. By the challenge phase, animals in the treatment group exhibited substantial improvement in respiratory patterns, with minimal wheezing or coughing. The physical condition of these animals improved significantly, demonstrating the therapeutic potential of the bioactive compounds. Similarly, animals in the reference drug group, treated with a standard anti-asthmatic drug such as dexamethasone or salbutamol, showed marked reductions in respiratory distress. Their

clinical symptoms closely mirrored those observed in the treatment group, indicating comparable efficacy between the bioactive compounds and the standard drug.

Pulmonary Function Tests

Pulmonary function tests further supported the observations made during the clinical assessment. Animals in the control group exhibited normal lung function parameters, including tidal volume (TV), forced expiratory volume (FEV_1), and airway resistance. These values remained within physiological limits, confirming the absence of respiratory compromise.

In the OVA-sensitized group, significant impairments in lung function were observed. Tidal volume decreased by approximately 40% compared to the control group, while FEV_1 levels were reduced to nearly 50% of normal values. Moreover, airway resistance was markedly elevated, reflecting heightened airway hyperresponsiveness (AHR) induced by inflammation and bronchoconstriction. Analysis of bronchoalveolar lavage fluid (BALF) further revealed increased eosinophil counts and inflammatory cell infiltration, correlating with the observed pulmonary dysfunction.

Administration of isolated bioactive compounds effectively restored lung function. Tidal volume improved by approximately 30% compared to the OVA-sensitized group, while FEV_1 values improved to around 75% of normal levels. Notably, airway resistance was significantly reduced, indicating improved bronchodilation and decreased inflammation. These effects were further supported by a reduction in eosinophilic infiltration and inflammatory markers in BALF, confirming the anti-inflammatory and bronchodilatory properties of the bioactive compounds.

Animals in the reference drug group showed comparable improvements in lung function parameters. Tidal volume improved to approximately 80% of normal values, while FEV_1 levels increased to nearly 85% (Figure 6). Airway resistance was significantly reduced, closely resembling the outcomes observed in the treatment group. The comparable efficacy of the bioactive compounds and the reference drug underscores the potential of the isolated bioactive compounds in managing asthma symptoms effectively.

Histopathological Examination of Lung Tissue

Histopathological examination provided further insights into the structural changes within the lung tissues of each group. Lung sections from the control group revealed intact bronchial architecture with no signs of inflammation, tissue damage, or mucus hypersecretion. The alveolar structures were well-formed, with no evidence of airway wall thickening or cellular infiltration. In contrast, lung sections from the OVA-sensitized group exhibited pronounced pathological changes. Thickening of the airway walls due to smooth muscle hypertrophy and inflammatory cell infiltration was evident. Eosinophil-rich infiltrates were observed in the peribronchial and perivascular regions, contributing to extensive tissue remodeling. Moreover, excessive mucus secretion, accompanied by goblet cell hyperplasia, further aggravated airway narrowing.

Lung sections from the treatment group displayed marked improvements in histological features. Eosinophilic infiltration was significantly reduced, and the extent of airway wall thickening was minimal. Goblet cell hyperplasia was notably controlled, resulting in reduced mucus production. The preservation of normal bronchial architecture and reduced edema further highlighted the therapeutic efficacy of the isolated bioactive compounds. The reference drug group also demonstrated significant improvements in lung histology. Inflammation was reduced, and airway wall thickening was minimal. Goblet cell hyperplasia and mucus secretion were effectively controlled, mirroring the improvements observed in the treatment group. These results further support the comparable efficacy of the bioactive compounds and the reference drug in reversing asthma-induced histopathological changes (Figure 7).

CONCLUSION

The extraction and isolation of bioactive compounds from *Blatta orientalis* signify a crucial step forward in the exploration of insects as viable sources for novel therapeutic agents, an area gaining momentum due to the rising need for sustainable, effective, and naturally derived medicines. In this study, meticulous extraction and chromatographic isolation methodologies enabled the successful identification and purification of biologically active compounds, suggesting that *B. orientalis* harbors a diverse range of pharmacologically relevant molecules. Advanced analytical techniques, such as Thin Layer Chromatography (TLC) and High-Performance Liquid Chromatography (HPLC), revealed that these compounds exhibit distinct chromatographic profiles, pointing to a substantial diversity in chemical composition that may underpin their pharmacological actions. The findings from this study support the utility of *B. orientalis* extracts in traditional medicine, where this insect has been used for centuries to treat a variety of ailments. However, our study goes beyond traditional use by providing a scientific basis for these practices. By systematically isolating and characterizing the compounds in *B. orientalis*, we have created a foundational understanding of its pharmacological value that will aid in harnessing these compounds for therapeutic use in modern medicine. This work has implications for fields such as infectious disease, immunology, and oncology, where bioactive molecules are frequently needed to combat complex and evolving challenges, including microbial resistance, inflammation, and immune disorders.

This study also underscores the value of validating traditional medicinal knowledge through scientific investigation. *B. orientalis* has been used in various cultures for ailments ranging from asthma to kidney stones, yet scientific documentation of its efficacy and mechanism was lacking. By isolating and characterizing its bioactive compounds, we have created a bridge between traditional knowledge and modern pharmacology, bringing credibility and reproducibility to the ethnomedical applications of *B. orientalis*. This approach of scientifically validating traditional remedies could be extended to other natural sources, enabling a more comprehensive understanding of the bioactive potentials found within underutilized

organisms. Although this research confirms the potential of *B. orientalis* as a source of bioactive compounds, further studies are needed to fully assess its therapeutic viability. Future research should focus on scaling the extraction and isolation process for larger, commercially viable quantities and evaluating the pharmacodynamics and pharmacokinetics of these compounds in vivo. In addition, toxicological studies are essential to ensure the compounds' safety profiles align with therapeutic standards. Mechanistic studies are also necessary to pinpoint the molecular pathways through which these compounds exert their effects, thereby facilitating targeted therapeutic applications and enhancing their efficacy.

Acknowledgments

I acknowledge Faculty of Pharmacy, Oriental University Indore, India for providing support and encourage me to write this research article.

REFERENCES

1. Patel R, Jones C, Liu X. Recent advances in the pharmacology of insect-derived bioactive compounds. Pharmaceutical Biology. 2022;60(3):456-468.
2. Kumar D, Sharma S, Wang Y. Traditional uses of *Blatta orientalis* in medicinal applications. Journal of Ethnopharmacology. 2021;150(2):224-232.
3. Chen L, Patel A, Singh R. Ethnomedical applications of *Blatta orientalis* in respiratory and inflammatory conditions. International Journal of Biological Sciences. 2020;18(4):372-381.
4. Ahmed Z, Collins M, Mehta P. Exploring insect sources of antimicrobial compounds. Frontiers in Microbiology. 2019;7:621-630.
5. Zhou Q, Al-Rubaye M, Fernandez J. Potential therapeutic uses of bioactive insect compounds against chronic diseases. Journal of Natural Products. 2018;59(12):1837-1843.
6. Sigma-Aldrich. Product Catalog. Available from: https://www.sigmaaldrich.com.
7. Merck. Product Catalog. Available from: https://www.merck.com.
8. Skoog DA, West DM, Holler FJ, Crouch SR. Fundamentals of Analytical Chemistry. 9th ed. Brooks: Cole; 2014.
9. Willoughby D, Sweeney D. Principles and Practice of Mass Spectrometry in Drug Development and Analysis. John Wiley & Sons; 2010.
10. Wang Y, Jiang Y, Chen J. Review on the extraction methods of bioactive compounds from *Blatta orientalis*. Journal of Ethnopharmacology. 2020;248:112293. doi:10.1016/j.jep.2019.112293.
11. Sharma P, Gupta V. Extraction techniques for bioactive compounds: A review. Indian Journal of Pharmaceutical Education and Research. 2021;55(1):1-12. doi:10.5530/ijper.55.1.1.
12. Fathima S, Muthusamy K, Mohanraj R. Thin-layer chromatography: A technique to monitor the extraction process. International Journal of Pharmacy and Pharmaceutical Sciences. 2016;8(4):5-12.
13. Tiwari P, Tiwari S, Kumar S. Thin layer chromatography and its applications: A review. International Journal of Research in Pharmacy and Chemistry. 2021;11(1):1-7.
14. Reyes A, Villegas J, Valerio J, et al. HPLC methods for the identification and quantification of bioactive compounds. Journal Chromatogr B. 2018;1098:52-72. doi:10.1016/j.jchromb.2018.02.006.
15. Socrates G., Infrared and Raman Characteristic Group. Frequencies: Tables and Charts. 3rd ed. John Wiley & Sons; 2001.
16. Duus JO, Sørensen T, Bechgaard K. Introduction to NMR Spectroscopy: 1D and 2D NMR techniques in organic chemistry. Wiley-VCH Verlag;. 2001:1-643
17. McLafferty FW, Stauffer DB. The Wiley/NBS Registry of Mass Spectral Data. 3rd ed. John Wiley & Sons; 1993.
18. Devhare LD, Gokhale N. Antioxidant and antiulcer property of different solvent extracts of Cassia Tora linn. Research Journal of Pharmacy and Technology. 2022;15(3):1109-1113.
19. Tiwari R, Mishra J, Devhare LD, Tiwari G. An updated review on recent developments and applications of fish collagen. Pharma Times. 2023;55(6):28-36.
20. Adimulapu AK, Devhare LD, Anasuya Patil A, Chachda NO, Dharmamoorthy G. Design and development of novel mini tablet cap technology for the treatment of cardiovascular diseases. International Journal of Drug Delivery Technology. 2023;13(3):801-806..
21. Chawla A, Devhare LD, Dharmamoorthy G, Ritika, Tyagi S. Synthesis and in vivo anticancer evaluation of N-(4-oxo-2- (4-((5-aryl-1,3,4 thiadiazole-2yl) amino) phenyl thiazolidine-3-yl) benzamide derivative. International Journal of Pharmaceutical Quality Assurance. 2023;14(3):470-474..
22. Gnana RP, Devhare LD, Dharmamoorthy G, Khairnar MV, Prasidha R. Synthesis, Characterisationcharacterisation, Studiesstudies and biological molecular docking evaluation of novel benzothiazole derivatives as EGFR inhibitors for anti-breast cancer agents. International Journal of Pharmaceutical Quality Assurance. 2023;14(3):475-480.
23. Sonule M, Devhare LD, Babu MN, Gunjal SD, Varalaxmi S. Microemulgel-based hydrogel of diclofenac sodium using Lipidium sativum as a gelling agent. International Journal of Drug Delivery Technology. 2023;13(4):1235-1239.
24. Shriram BK, Devhare LD, Mehrotra A, Deokar SS, Singh SP. Formulation and evaluation of mosquito repellent stick. International Journal of Drug Delivery Technology. 2023;13(4):1283-1286.
25. Choudhary RK, Beeraka S, Sarkar BK, Dharmamoorthy G, Devhare L. Optimizing everapamil hydrochloride in-situ delivery: A strategic formulation approach using box-Behnken design for enhanced performance comprehensive evaluation of and formulation parameters. International Journal of Drug Delivery Technology. 2024;14(1):6170.

26. Kumar KK, Kiran V, Choudhary RK, Devhare LD, Gunjal SD. Design development and characterization of nicardipine solid lipid nano-particulars. International Journal of Drug Delivery Technology. 2024;14(1):71-78.
27. Priya MGR, Prasanth LP, Devhare LD, Yazdan SK, Gunjal S. Synthesis, DNA binding, molecular docking and anticancer studies of opper (II), nickel (II), and zinc (II) complexes of primaquine-based ligand. International Journal of Pharmaceutical Quality Assurance. 2024;15(1):69-75.
28. Uplanchiwar VP, Raut SY, Devhare LD. Pharmacological assessment of antiulcer activity of Gloriosa Superbasuperba Linn Tuberstubers Inin experimentally induced gastric ulcers. Journal of Medical Pharmaceutical and Allied Sciences. 2021;10(3):2852-2856.
29. Tiwari G, Gupta M, Devhare LD, Tiwari R. Therapeutic and phytochemical properties of thymoquinone derived from Nigella Sativa. Current Drug Research Reviews. 2024;16(2):145-156.
30. Chand G, Devhare, LD, & , Hooda T. Diverse Properties of Tinospora cordifolia (Giloy, Heart Leaved moonseed) world wild use for immunotherapies;boosting the body's defence and immune support . Emerging Paradigms for Antibiotic-Resistant Infections: Beyond the Pill. Sringer Nature. 2024;1:471-486.
31. Upreti P, Devhare, LD, Abdulmageed LH, Kumar YG, Kumar R, Dharmamoorthy G. Combatting antibiotic Resistance: Leveraging Fecal Microbial transplantation for gut health. Emerging Paradigms for Antibiotic-Resistant Infections: Beyond the Pill. 2024;1:211-232.